JCTC Journal of Chemical Theory and Computation

Article

pubs.acs.org/JCTC

Long-Range Corrected Hybrid Density Functionals with Improved Dispersion Corrections

You-Sheng Lin,[†] Guan-De Li,[†] Shan-Ping Mao,[†] and Jeng-Da Chai*[,†,‡]

[†]Department of Physics, National Taiwan University, Taipei 10617, Taiwan

[‡]Center for Theoretical Sciences and Center for Quantum Science and Engineering, National Taiwan University, Taipei 10617, Taiwan

Supporting Information

ABSTRACT: By incorporating the improved empirical atom−atom dispersion corrections from DFT-D3 [Grimme, S.; Antony, J.; Ehrlich, S.; Krieg, H. *J. Chem. Phys.* **2010**, *132*, 154104], two long-range corrected (LC) hybrid density functionals are proposed. Our resulting LC hybrid functionals, ωM06-D3 and ωB97X-D3, are shown to be accurate for a very wide range of applications, such as thermochemistry, kinetics, noncovalent interactions, frontier orbital energies, fundamental gaps, and long-range charge-transfer excitations, when compared with common global and LC hybrid functionals. Relative to ωB97X-D [Chai, J.-D.; Head-Gordon, M. *Phys. Chem. Chem. Phys.* **2008**, *10*, 6615], ωB97X-D3 (reoptimization of ωB97X-D with improved dispersion corrections) is shown to be superior for nonbonded interactions, and similar in performance for bonded interactions, while ωM06-D3 is shown to be superior for general applications.

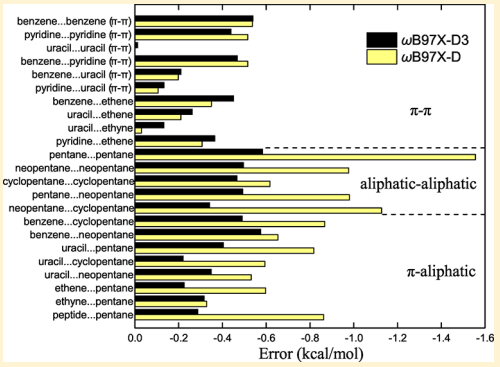

1. INTRODUCTION

Over the past two decades, Kohn−Sham density functional theory (KS-DFT)[1,2] has become one of the most popular methods for the study of large ground-state systems, owing to its favorable balance between accuracy and efficiency.[3−6] Its extension for treating electron dynamics and excited-state systems, time-dependent density functional theory (TDDFT), has also been actively developed and widely applied.[7,8]

In KS-DFT, the exact exchange-correlation (XC) energy functional $E_{xc}[\rho]$ remains unknown and needs to be approximated. Accurate density functional approximations to $E_{xc}[\rho]$ have been successively developed to extend the applicability of KS-DFT to a wide range of systems.[9,10] Among them, semilocal density functionals perform satisfactorily for some applications but can produce erroneous results in situations where the accurate treatment of nonlocality of the XC hole is important.[11,12]

Aiming to include nonlocality of the XC hole into $E_{xc}[\rho]$, the important role of Hartree−Fock (HF) exchange in $E_{xc}[\rho]$ was demonstrated by Becke, based on the adiabatic connection argument and numerical support.[13] Thereafter, the hybrid DFT method, combining a fraction of HF exchange with a semilocal density functional, has gradually gained popularity. However, in certain situations, especially in the asymptotic regions of molecular systems, a large fraction (even 100%) of HF exchange is needed. Commonly used hybrid functionals, such as B3LYP,[13,14] do not qualitatively resolve these problems.

To date, perhaps the most successful approach in practice to include nonlocal exchange effects for finite systems is provided by the long-range corrected (LC) hybrid method,[15−28] employing 100% HF exchange for the long-range (LR) part of the interelectron repulsion operator $\mathrm{erf}(\omega r_{12})/r_{12}$, a semilocal exchange density functional for the complementary short-range (SR) operator $\mathrm{erfc}(\omega r_{12})/r_{12}$, and a semilocal correlation density functional, with the parameter ω defining the partitioning of the interelectronic distance r_{12}. One of the important issues in the LC hybrid method is the development of an accurate SR semilocal exchange density functional going beyond the simple local density approximation.[29] Particularly, several schemes have been proposed to generate a SR semilocal exchange density functional based on a given semilocal exchange density functional.[15,19,23,28] Recently, we have developed an accurate scheme, yielding a reliable LC hybrid functional for a wide range of applications.[28]

Since the correlation density functionals in typical LC hybrids are treated semilocally, there are still problems associated with the lack of dispersion interactions (the missing of van der Waals (vdW) forces).[30] Currently, perhaps the most popular approach in practice to include the effects of dispersion interactions is provided by the DFT-D (density functional theory with empirical dispersion corrections) method, due to its low cost and robust performance on various noncovalent systems.[31] Recently, Grimme and co-workers have proposed an improved DFT-D method, denoted as DFT-D3.[32] In DFT-D3, the atom-pairwise dispersion coefficients and cutoff radii are computed from first principles to reduce the empiricism, and the coefficients of the eighth-order dispersion terms are

Received: August 14, 2012
Published: November 5, 2012

computed using the established recursion relations. For the first time in the DFT-D methods, the atomic-pairwise dispersion coefficients are dependent on system geometry (as they should be). By labeling the calculated coefficients with fractional coordination numbers (CN) calculated by a well-designed function taking the molecular geometry as input, a dispersion coefficient is interpolated between dispersion coefficients in different reference chemical environments.

We emphasize that both of the two methods may be simultaneously needed in some situations, such as intermolecular charge-transfer excitations of dispersion-bound complexes. Therefore, to develop density functionals that are computationally efficient and generally accurate, in this work, we propose two LC hybrid functionals with the improved dispersion corrections from DFT-D3. Our results are compared with three closely related functionals on diverse test sets.

2. LC HYBRID FUNCTIONALS WITH IMPROVED DISPERSION CORRECTIONS

2.1. ωM06-D3. The M06-class functionals[33−35] share a common functional form, which can be expressed as a linear combination of the M05[36,37] and VSXC[38] functional forms. Among them, M06-2X[33] is the only one without using the VSXC exchange. Nevertheless, M06-2X performs well for many applications and remains outstanding among the M06-class functionals. Therefore, one of our proposed LC hybrid functionals, denoted as ωM06-D3, is based on modification of M06-2X (a global hybrid functional).

Following our recently developed scheme,[28] the SR semilocal exchange density functional in ωM06-D3 is denoted as SR-M06, as it reduces to the M06-2X exchange at $\omega = 0$.

$$E_x^{\mathrm{SR-M06}} = \sum_\sigma \int e_{x\sigma}^{\mathrm{SR-PBE}}(\rho_\sigma, \nabla\rho_\sigma)\, f(w_\sigma)\, \mathrm{d}\mathbf{r} \tag{1}$$

where $e_{x\sigma}^{\mathrm{SR-PBE}}(\rho_\sigma,\nabla\rho_\sigma)$ is the SR-PBE exchange energy density[39] ($\sigma = \alpha$ for spin up or β for spin down) and $f(w_\sigma)$ is the kinetic-energy-density enhancement factor:

$$f(w_\sigma) = \sum_{i=0}^{m} a_i w_\sigma^i \tag{2}$$

Here, w_σ is given by

$$w_\sigma = (t_\sigma - 1)/(t_\sigma + 1) \tag{3}$$

where

$$t_\sigma = \tau_\sigma^{\mathrm{LDA}}/\tau_\sigma \tag{4}$$

with

$$\tau_\sigma = \frac{1}{2}\sum_i^{\mathrm{occ.}} |\nabla\psi_{i\sigma}|^2 \tag{5}$$

being the KS spin kinetic energy density ($\psi_{i\sigma}$ are the occupied KS orbitals) and

$$\tau_\sigma^{\mathrm{LDA}} = \frac{3}{10}(6\pi^2)^{2/3}\rho_\sigma^{5/3} \tag{6}$$

being the LDA spin kinetic energy density.

We use the same form for the correlation functional as the M06[33] (or M06-2X) correlation functional, which includes terms in the VSXC functional, involving the dimensionless reduced spin density gradient $s_\sigma \equiv |\nabla\rho_\sigma|/\rho_\sigma^{4/3}$, the variable $z_\sigma \equiv 3/5\ (6\pi^2)^{2/3}(1 - t_\sigma)/t_\sigma$, and two functions y and h:

$$y(s_\sigma^2, z_\sigma) = 1 + b(s_\sigma^2 + z_\sigma) \tag{7}$$

$$h(s_\sigma^2, z_\sigma) = \frac{d_0}{y(s_\sigma^2, z_\sigma)} + \frac{d_1 s_\sigma^2 + d_2 z_\sigma}{y^2(s_\sigma^2, z_\sigma)} + \frac{d_3 s_\sigma^4 + d_4 s_\sigma^2 z_\sigma + d_5 z_\sigma^2}{y^3(s_\sigma^2, z_\sigma)} \tag{8}$$

where b, d_0, d_1, d_2, d_3, d_4, and d_5 are parameters to be determined. The M06 correlation functional can be decomposed into same-spin $E_{c\sigma\sigma}^{\mathrm{M06}}$ and opposite-spin $E_{c\alpha\beta}^{\mathrm{M06}}$ components

$$E_c^{\mathrm{M06}} = \sum_\sigma E_{c\sigma\sigma}^{\mathrm{M06}} + E_{c\alpha\beta}^{\mathrm{M06}} \tag{9}$$

For the opposite-spin terms,

$$E_{c\alpha\beta}^{\mathrm{M06}} = \int e_{c\alpha\beta}^{\mathrm{LDA}}[g_{\alpha\beta}(s_{\alpha\beta}^2) + h_{\alpha\beta}(s_{\alpha\beta}^2, z_{\alpha\beta})]\, \mathrm{d}\mathbf{r} \tag{10}$$

$$g_{\alpha\beta}(s_{\alpha\beta}^2) = \sum_{i=0}^{n} c_{\alpha\beta,i}\left[\frac{\gamma_{\alpha\beta}s_{\alpha\beta}^2}{1 + \gamma_{\alpha\beta}s_{\alpha\beta}^2}\right]^i \tag{11}$$

and $h_{\alpha\beta}(s_{\alpha\beta}^2,z_{\alpha\beta})$ is defined in eq 8, with $s_{\alpha\beta}{}^2 \equiv s_\alpha{}^2 + s_\beta{}^2$ and $z_{\alpha\beta} \equiv z_\alpha + z_\beta$. For the same-spin terms,

$$E_{c\sigma\sigma}^{\mathrm{M06}} = \int e_{c\sigma\sigma}^{\mathrm{LDA}}[g_{\sigma\sigma}(s_\sigma^2) + h_{\sigma\sigma}(s_\sigma^2, z_\sigma)]D_\sigma\, \mathrm{d}\mathbf{r} \tag{12}$$

$$g_{\sigma\sigma}(s_\sigma^2) = \sum_{i=0}^{n} c_{\sigma\sigma,i}\left[\frac{\gamma_{\sigma\sigma}s_\sigma^2}{1 + \gamma_{\sigma\sigma}s_\sigma^2}\right]^i \tag{13}$$

$h_{\sigma\sigma}(s_\sigma^2,z_\sigma)$ is defined in eq 8, and D_σ is a self-interaction correction factor proposed by Becke[40]

$$D_\sigma = 1 - \frac{|\nabla\rho_\sigma|^2}{8\rho_\sigma\tau_\sigma} \tag{14}$$

which vanishes for any one-electron system. The correlation energy densities $e_{c\alpha\beta}^{\mathrm{LDA}}$ and $e_{c\sigma\sigma}^{\mathrm{LDA}}$ are derived from the Perdew−Wang parametrization of the LDA correlation energy,[41] using the approach of Stoll et al.[42] The values of the nonlinear parameters in $g_{\alpha\beta}(s_{\alpha\beta}^2)$ and $g_{\sigma\sigma}(s_\sigma^2)$ are taken from ref 36:

$$\gamma_{\alpha\beta} = 0.0031,\ \gamma_{\sigma\sigma} = 0.06 \tag{15}$$

and the values of the nonlinear parameters in $h_{\alpha\beta}(s_{\alpha\beta}^2,z_{\alpha\beta})$ and $h_{\sigma\sigma}(s_\sigma^2,z_\sigma)$ are taken from ref 38:

$$b_{\alpha\beta} = 0.00304966,\ b_{\sigma\sigma} = 0.00515088 \tag{16}$$

On the basis of the above functional expansions, the functional form of ωM06-D3 can be written as

$$E_{\mathrm{xc}}^{\omega\mathrm{M06\text{-}D3}} = E_x^{\mathrm{LR\text{-}HF}} + c_x E_x^{\mathrm{SR\text{-}HF}} + E_x^{\mathrm{SR\text{-}M06}} + E_c^{\mathrm{M06}} \tag{17}$$

where $E_{\mathrm{x}}^{\mathrm{LR-HF}}$ is the LR HF exchange, $E_x^{\mathrm{SR-HF}}$ is the SR HF exchange, and c_x is the fraction of SR HF exchange.

The exact uniform electron gas (UEG) limit for ωM06-D3 is enforced by imposing the following constraints:

$$c_{\alpha\beta,0} + d_{\alpha\beta,0} = 1 \tag{18}$$

$$c_{\sigma\sigma,0} + d_{\sigma\sigma,0} = 1 \tag{19}$$

and

$$a_0 + c_x = 1 \tag{20}$$

dx.doi.org/10.1021/ct300715s | J. Chem. Theory Comput. 2013, 9, 263−272

Table 1. Optimized Parameters for ωM06-D3 and ωB97X-D3[a]

ωM06-D3		ω	c_x	$s_{r,6}$	
		0.30 bohr^{-1}	0.271519	1.510	
i	a_i	$c_{\alpha\beta,i}$	$c_{\sigma\sigma,i}$	$d_{\alpha\beta,i}$	$d_{\sigma\sigma,i}$
0	0.728481	9.81364	−7.39562	−8.81364	8.39562
1	−0.203715	−14.3222	−6.34101	0.011233	0.140716
2	0.0851649	15.7139	10.2807	−0.0398094	0.0895217
3	1.60545	−18.1878	−8.83082		
4	−3.70366				
5	−6.78298				
6	21.8665				
7	11.3064				
8	−42.5053				
9	−7.41299				
10	27.0693				
ωB97X-D3		ω	c_x	$s_{r,6}$	$s_{r,8}$
		0.25 bohr^{-1}	0.195728	1.281	1.094
i	$c_{x\sigma,i}$	$c_{c\alpha\beta,i}$	$c_{c\sigma\sigma,i}$		
0	0.804272	1.000000	1.000000		
1	0.698900	2.433266	−4.868902		
2	0.508940	−15.446008	21.295726		
3	−3.744903	17.644390	−36.020866		
4	10.060790	−8.879494	19.177018		

[a]Here, the nonlinear parameters $s_{r,6}$ and $s_{r,8}$ are defined in eq 23, while other parameters of ωM06-D3 are defined in eq 17, and those of ωB97X-D3 use the same notations as the parameters of ωB97X-D.[24]

Following the general form of the DFT-D method,[31] our total energy is given by

$$E_{\text{DFT-D}} = E_{\text{KS-DFT}} + E_{\text{disp}} \tag{21}$$

which is the sum of a KS-DFT part and an empirical atomic-pairwise dispersion correction (three-body dispersion contributions are not included) from DFT-D3.[32] We choose to use an unscaled dispersion correction given by

$$E_{\text{disp}} = -\frac{1}{2}\sum_{n=6,8}\sum_{AB}\frac{C_n^{AB}(\text{CN}^A, \text{CN}^B)}{R_{AB}^n} f_{d,n}(R_{AB}) \tag{22}$$

Here, the second sum is over all atom pairs in the system, and R_{AB} is the interatomic distance of atom pair AB. The conditions of zero dispersion correction at short interatomic distances and correct asymptotic pairwise vdW potentials are enforced by the damping functions

$$f_{d,n}(R_{AB}) = \frac{1}{1 + 6(s_{r,n}R_0^{AB}/R_{AB})^{\alpha_n}} \tag{23}$$

where $\alpha_6 = 14$ and $\alpha_8 = 16$. In DFT-D3, a sophisticated approach to obtain the cutoff radius R_0^{AB} is proposed,[32] whereby a total of 4465 values are precomputed for all atom pairs AB constituted by the first 94 elements of the periodic table.

In eq 22, CN^A is a fractional coordination number of atom A, calculated as the sum of a distance-dependent "counting" function over other atoms in the system. $C_6^{AB}(\text{CN}^A,\text{CN}^B)$ is a function to perform two-dimensional interpolation from a few precomputed dispersion coefficients $C_{6,\text{ref}}^{AB}(\text{CN}_i^A,\text{CN}_j^B)$, where CN_i^A is the coordination number of atom A in reference system i. Because every element in the periodic table forms a stable hydride (except for the rare gases), the reference systems are chosen to be the atoms and the hydrides A_mH_n. By performing computations over the reference systems, CN_i^A and $C_{6,\text{ref}}^{AB}(\text{CN}_i^A,\text{CN}_j^B)$ are published for the elements up to $Z = 94$.[32]

The eighth-order dispersion coefficients are computed according to the established recursion relations

$$C_8^{AB} = 3C_6^{AB}\sqrt{Q^AQ^B} \tag{24}$$

where

$$Q = s_{42}\sqrt{Z}\frac{\langle r^4\rangle}{\langle r^2\rangle} \tag{25}$$

In eq 25, $\langle r^4\rangle$ and $\langle r^2\rangle$ are simple multipole-type expectation values derived from atomic densities. The value of the factor s_{42} has been chosen such that reasonable C_8^{AA} values for He, Ne, and Ar are obtained.[32]

As can be seen in eq 22, $s_{r,6}$ and $s_{r,8}$, the scaling factors of the cutoff radii R_0^{AB}, are the only parameters to be determined for the strength of the dispersion corrections of ωM06-D3.

2.2. ωB97X-D3. As a possible improvement of ωB97X-D[24] for noncovalent systems, we replace the original dispersion corrections of ωB97X-D with the improved dispersion corrections from DFT-D3 (see eq 22) and reoptimize the new functional on the same training set of ωB97X-D. The resulting LC hybrid functional is denoted as ωB97X-D3.

2.3. Systematic Optimization. We determined the optimal ω values, the $s_{r,6}$ and $s_{r,8}$ values, the linear expansion coefficients, and the expansion orders of ωM06-D3 and ωB97X-D3 by least-squares fittings to the same diverse training set described in ref 23, which contains 412 accurate experimental and accurate theoretical results, including the 18 atomic energies from the H atom to the Ar atom,[43] the 223 atomization energies of the G3/99 set,[44−46] the 40 ionization potentials (IPs), 25 electron affinities (EAs), eight proton affinities (PAs) of the G2-1 set,[47] the 76 barrier heights of the NHTBH38/04 and HTBH38/04 sets,[48,49] and the 22 noncovalent interactions of the S22 set.[50−52] For the interaction energies of the S22 set,[50] we adopt an updated version of reference values from S22A.[51] The S22 data are weighted 10

dx.doi.org/10.1021/ct300715s | J. Chem. Theory Comput. 2013, 9, 263−272

Table 2. Statistical Errors (in kcal/mol) of the Training Set[a]

system	error	ωM06-D3	ωB97X-D3	ωB97X-D	ωM05-D	M06-2X
atoms	MSE	0.22	−0.17	−0.05	0.37	4.95
(18)	MAE	2.17	1.64	2.51	2.02	5.07
G3/99	MSE	0.07	−0.14	−0.24	−0.03	0.40
(223)	MAE	1.62	2.05	1.93	1.62	2.32
IP	MSE	−0.24	0.06	0.19	−0.80	0.16
(40)	MAE	2.44	2.66	2.74	2.86	2.45
EA	MSE	−0.39	−0.36	0.07	−1.02	−1.37
(25)	MAE	1.92	1.92	1.91	2.12	2.56
PA	MSE	−0.62	1.09	1.42	−1.48	−1.21
(8)	MAE	1.84	1.29	1.50	2.10	2.02
NHTBH	MSE	0.18	0.04	−0.45	−0.94	0.00
(38)	MAE	1.40	1.53	1.51	1.57	1.41
HTBH	MSE	−1.54	−2.08	−2.57	−2.82	−0.81
(38)	MAE	2.08	2.40	2.70	2.83	1.32
S22	MSE	0.00	−0.06	−0.12	−0.05	0.22
(22)	MAE	0.20	0.17	0.20	0.34	0.39
all	MSE	−0.14	−0.27	−0.37	−0.52	0.28
(412)	MAE	1.69	1.96	1.96	1.84	2.18

[a]M06-2X was not particularly parametrized using this training set.

times more than the others. All the parameters in ωM06-D3 and ωB97X-D3 are self-consistently determined by a least-squares fitting procedure described in ref 23. For the nonlinear parameter optimization, we focus on a range of possible ω values (0.00, 0.05, 0.10, 0.15, 0.20, 0.25, 0.30, 0.35, and 0.40 Bohr^{-1}) and optimize the corresponding $s_{r,6}$ and $s_{r,8}$ values with suitable steps.

During the optimization procedure, we truncate the functional expansions of ωM06-D3 and ωB97X-D3, when their statistical errors of the training set are not significantly improved. Truncation of redundant terms does not make much difference in the training-set results but can avoid the occurrence of large parameters which increases the possibility of convergence difficulty as well as overfitting effects. The last VSXC term in eq 8 is found to be insignificant and is discarded (i.e., we set $d_3 = d_4 = d_5 = 0$) from ωM06-D3. Besides, the eighth-order term of the dispersion energy (see eq 22) is also found to be insignificant and thus discarded for ωM06-D3. This may be related to the fact that the M06-class functionals[33−35] are capable of describing the middle-range correlation effects correctly. Therefore, double-counting effects and deteriorating results may occur when the eighth-order term is included in ωM06-D3. This treatment also agrees with previous work,[53] when combining the M06-class functionals with DFT-D3. By contrast, both the sixth-order and eighth-order terms of the dispersion energy (see eq 22) are found to be significant for ωB97X-D3 and are retained.

The optimized parameters of ωM06-D3 and ωB97X-D3 are summarized in Table 1. Relative to ωB97X-D,[24] ωB97X-D3 adopts a slightly larger ω (= 0.25 Bohr^{-1}) and a slightly smaller fraction of SR-HF exchange c_x (≈ 0.20), while ωM06-D3 adopts a larger ω (= 0.30 Bohr^{-1}) and a larger c_x (≈ 0.27), which helps to reduce the self-interaction error of the functional, as will be seen later.

The overall performance of our new LC hybrid functionals, ωM06-D3 and ωB97X-D3, will be compared with three closely related functionals, including the popular global hybrid functional M06-2X,[33] our previous LC hybrid functional ωM05-D,[28] and the popular LC hybrid functional ωB97X-D.[24]

3. RESULTS FOR THE TRAINING SET

All calculations are performed with a development version of Q-CHEM 3.2.[54] Spin-restricted theory is used for singlet states and spin-unrestricted theory for others, unless noted otherwise. For the binding energies of the weakly bound systems, the counterpoise correction[55] is employed to reduce basis set superposition error (BSSE).

Results for the training set are computed using the 6-311++G(3df,3pd) basis set with the fine grid EML(75,302), consisting of 75 Euler-Maclaurin radial grid points[56] and 302 Lebedev angular grid points.[57] Boese and co-workers have studied the role of basis sets in density functional theory and recommended the large Pople type basis sets (or the triple-ζ basis set level) for calculations using semilocal density functionals or hybrid functionals.[58] Therefore, the 6-311++G(3df,3pd) basis set, which is the largest Pople type basis set, should suffice for most of the calculations in this work. The error for each entry is defined as error = theoretical value − reference value. The notation used for characterizing statistical errors is as follows: mean signed errors (MSEs), mean absolute errors (MAEs), and root-mean-square (RMS) errors. We use the S22A[51] version of reference values for the noncovalent interactions in Table 2. The results examined against another updated version, S22B,[52] are given in Table S7 in the Supporting Information, from which one can see that the results are quite close.

In Table 2, a comparison between ωM06-D3 and ωM05-D reflects the effect of the improved functional form and dispersion corrections. Despite its inferior performance for the atomic energies, ωM06-D3 has a similar performance to ωM05-D for the numerous G3/99 atomization energies, and it outperforms ωM05-D for all other subsets to achieve the best overall training-set results. When compared with M06-2X, ωM06-D3 outperforms its popular predecessor for most subsets, except for the HTBH set, which is also included in the training set of M06-2X. A comparison between ωB97X-D3 and ωB97X-D reflects the effect of the improvement in dispersion corrections. Although ωB97X-D3 has a similar overall performance to ωB97X-D for the training set, it performs better for noncovalent interactions.

Table 3. Statistical Errors (in kcal/mol) of the Test Sets

system	error	ωM06-D3	ωB97X-D3	ωB97X-D	ωM05-D	M06-2X
G3/05	MSE	−0.61	0.61	0.25	−0.85	−2.84
(48)	MAE	2.88	3.09	3.02	3.21	5.08
RE	MSE	0.13	−0.16	−0.24	−0.58	−0.59
(30)	MAE	1.51	1.65	1.63	1.49	1.21
noncovalent	MSE	−0.06	−0.09	−0.14	−0.11	0.27
(29)	MAE	0.38	0.41	0.43	0.31	0.41
All	MSE	−0.25	0.20	0.01	−0.58	−1.37
(107)	MAE	1.82	1.96	1.93	1.94	2.73

Table 4. Statistical Errors (in kcal/mol) of the S66 Set[76]

system	error	ωM06-D3	ωB97X-D3	ωB97X-D	ωM05-D	M06-2X
hydrogen bonds	MSE	−0.07	−0.09	−0.04	0.18	0.33
(23)	MAE	0.15	0.14	0.16	0.22	0.34
dispersion	MSE	−0.50	−0.36	−0.58	−0.79	0.09
(23)	MAE	0.50	0.36	0.58	0.79	0.23
others	MSE	−0.14	−0.14	−0.18	−0.21	0.08
(20)	MAE	0.24	0.18	0.24	0.34	0.20
total	MSE	−0.24	−0.20	−0.27	−0.28	0.17
(66)	MAE	0.30	0.23	0.33	0.45	0.26

4. RESULTS FOR THE TEST SETS

To test the performance of ωM06-D3 and ωB97X-D3 outside the training set, we also evaluate their performance on various test sets, involving an additional 48 atomization energies of the G3/05 set,[59] the reaction energies of 30 chemical reactions (a test set described in ref 23), 29 noncovalent interactions (a test set described in ref 23), 66 noncovalent interactions of the S66 set,[60] four dissociation curves of symmetric radical cations, 131 vertical IPs, 115 vertical EAs, 115 fundamental gaps (FGs), and one long-range charge transfer excitation curve of two well-separated molecules. As discussed in ref 28, each EA can be evaluated in two different ways, and each FG can be evaluated in three different ways, so there are in total 884 pieces of data in the test sets, which are larger and more diverse than the training set. Unspecified detailed information of the test sets as well as the basis sets and numerical grids used is given in ref 23.

4.1. Atomization Energies, Reaction Energies, and Noncovalent Interactions. Table 3 summarized the general energetic results in the same way as in ref 24, for convenience of further comparisons. Since the 30 chemical reaction energies are taken from the NHTBH38/04 and HTBH38/04 databases calculated in Table 2, the EML(75,302) grid is used. Although ωM06-D3 has similar performance to ωM05-D for the atomization energies of the G3/99 set (see Table 2), its good performance for atomization energies seems transferable to the G3/05 set, which is a stringent test set containing third-row elements (none is included in the training set). ωM06-D3 has the best overall performance, followed by ωB97X-D, ωM05-D, and ωB97X-D3. Although M06-2X performs the best for the 30 reaction energies, it performs unsatisfactorily for the G3/05 set.

4.2. The S66 Set. Recently, the laboratory which developed the popular S22 set[50] presented a larger database of noncovalent interaction energies denoted as the S66 set.[60] The proposers have observed some problems in the S22 set. One potential problem is that S22 is heavily weighted toward nucleic-acid-like structures, containing many base-pair-like hydrogen bonds and many stacked aromatic species. However, the S22 set under-represents single hydrogen bonds and aromatic−aliphatic dispersion interactions and misses aliphatic−aliphatic dispersion interactions. The S66 set is designed to cover the most common types of noncovalent interactions in biomolecules, while keeping a balanced representation of dispersion and electrostatic contributions.

We evaluate the performance of the functionals using the 6-311++G(3df,3pd) basis set with the fine grid EML(75,302) and summarize the results in Table 4. As shown, the S66 set is divided into three categories: hydrogen bonding (23 complexes), dispersion-dominated (23), and "other" (20). ωB97X-D3 yields the best overall performance in the table and outperforms ωB97X-D in all three categories (especially for the dispersion category). Since ωB97X-D3 differs from ωB97X-D mainly in the versions of dispersion corrections, we plot their detailed results for the dispersion category in Figure 1. As illustrated, the dashed lines separate the three kinds of interactions: π−π, aliphatic−aliphatic, and π−aliphatic interactions. It is clear from the figure that ωB97X-D yields larger errors for more saturated aliphatic compounds involved, while ωB97X-D3 performs consistently well for all three kinds of

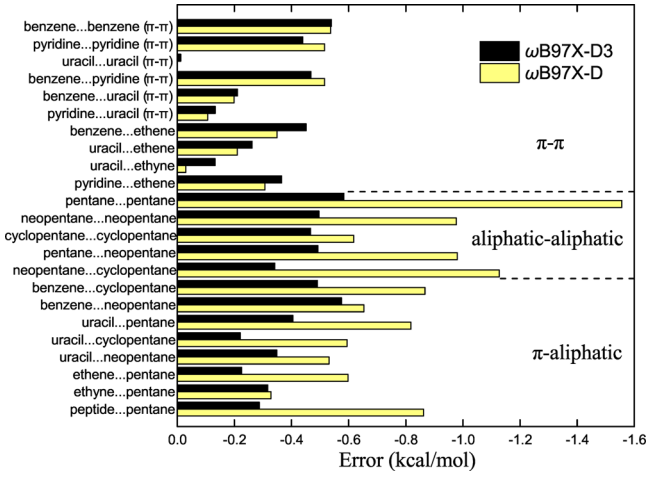

Figure 1. Comparison of errors of ωB97X-D3 and ωB97X-D for the dispersion category of the S66 set.[76]

Table 5. Summary of Statistical Errors (in kcal/mol) of All the Noncovalent Interactions Examined in the Present Work

database	error	ωM06-D3	ωB97X-D3	ωB97X-D	ωM05-D	M06-2X
S22	MSE	0.00	−0.06	−0.12	−0.05	0.22
(22)	MAE	0.20	0.17	0.20	0.34	0.39
noncovalent	MSE	−0.06	−0.09	−0.14	−0.11	0.27
(29)	MAE	0.38	0.41	0.43	0.31	0.41
S66	MSE	−0.24	−0.20	−0.27	−0.28	0.17
(66)	MAE	0.30	0.23	0.33	0.45	0.26
total	MSE	−0.15	−0.15	−0.21	−0.19	0.20
(117)	MAE	0.30	0.26	0.33	0.40	0.32

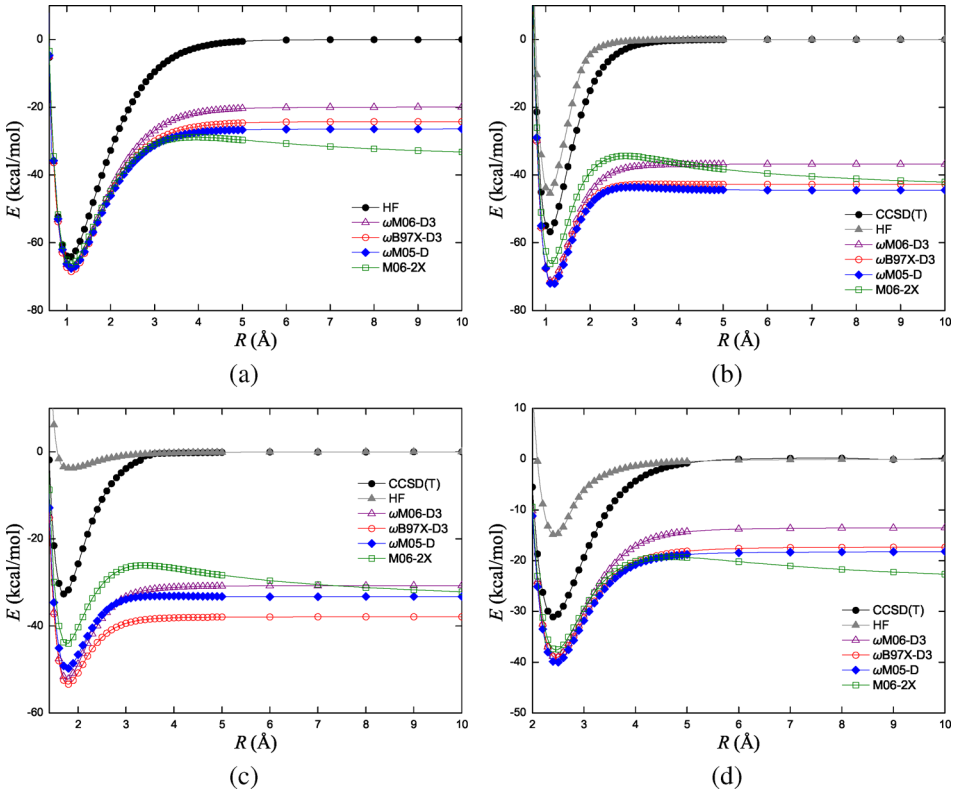

Figure 2. Dissociation curve of X_2^+, where X stands for H, He, Ne, and Ar in subfigures a, b, c, and d, respectively. Zero level is set to $E(X) + E(X^+)$ for each method.

interactions. Although M06-2X appears to perform the second best for the S66 set, due to the lack of $1/R^6$ corrections, M06-2X may miss dispersion forces between more distant pieces of larger molecules or in aggregates.

Recently, Vydrov and Van Voorhis have found that ωB97X-D assigns the dispersion coefficient C_6 = 30.4 au for all types of carbon−carbon interactions, but this value is too large for the less-polarizable saturated sp^3 carbon atoms.[61] By contrast, ωB97X-D3 adopts the dispersion corrections from DFT-D3, in which the dispersion coefficients depend on the system geometry, and C_6 = 18.1 au for interactions between saturated carbon atoms. Therefore, ωB97X-D3 consistently performs well for interactions involving aliphatic compounds in which the carbon atoms are in the sp^3 structure.

Table 5 summarizes all the noncovalent interactions examined, including the S22 set (in Table 2), the 29 noncovalent interactions (in Table 3), and the S66 set (in Table 4). In comparison with the other functionals, ωB97X-D3 consistently performs well for a wide range of noncovalent systems. Therefore, we recommend ωB97X-D3 as a balanced DFT approach for noncovalent interactions.

4.3. Dissociation of Symmetric Radical Cations. Due to the severe self-interaction errors (SIEs) of semilocal functionals, spurious fractional charge dissociation can occur,[22,62−64] especially for symmetric charged radicals X_2^+, such as H_2^+, He_2^+, Ne_2^+, and Ar_2^+. Gräfenstein and co-workers have obtained qualitatively correct results for these systems[65,66] using self-interaction-corrected DFT proposed by Perdew and Zunger[67] and confirmed that the deviations of standard DFT should be dominated by the SIEs.

To examine the performance of ωM06-D3 and ωB97X-D3 upon the SIE problem, we perform spin-unrestricted calculations using the aug-cc-pVQZ basis set and a high-quality EML(250,590) grid. The DFT results are compared with results from HF theory, and the very accurate CCSD(T) theory (coupled-cluster theory with iterative singles and doubles and perturbative treatment of triple substitutions).[68,69] For brevity, the binding curves of ωB97X-D are not shown here, as they can be found in ref 28. In Figure 2, we can see that LC hybrid functionals are essential to removing the unphysical barriers of the dissociation curves.[70] By contrast, the global hybrid functional M06-2X exhibits the undesirable X_2^+ dissociation

Table 6. Statistical Errors (in eV) of the Frontier Orbital Energies for the IP131 and EA115 Databases[28a]

system	error	ωM06-D3	ωB97X-D3	ωB97X-D	ωM05-D	M06-2X
			$-\varepsilon_N(N)-\mathrm{IP}_{\mathrm{vertical}}$			
atoms	MSE	−1.09	−1.37	−1.64	−1.48	−2.22
(18)	MAE	1.09	1.37	1.64	1.48	2.22
molecules	MSE	−0.28	−0.61	−0.92	−0.68	−1.37
(113)	MAE	0.35	0.62	0.92	0.68	1.37
total	MSE	−0.39	−0.72	−1.02	−0.79	−1.48
(131)	MAE	0.45	0.72	1.02	0.79	1.48
			$-\varepsilon_{N+1}(N+1)-\mathrm{EA}_{\mathrm{vertical}}$			
atoms	MSE	−0.20	−0.37	−0.53	−0.46	−1.32
(18)	MAE	0.36	0.44	0.57	0.49	1.32
molecules	MSE	−0.36	−0.43	−0.54	−0.55	−1.12
(97)	MAE	0.43	0.48	0.56	0.56	1.12
total	MSE	−0.34	−0.42	−0.54	−0.53	−1.15
(115)	MAE	0.42	0.48	0.56	0.55	1.15
			$-\varepsilon_{N+1}(N)-\mathrm{EA}_{\mathrm{vertical}}$			
atoms	MSE	−0.67	−0.21	−0.02	−0.27	0.77
(18)	MAE	0.81	0.65	0.74	0.73	1.00
molecules	MSE	−0.80	−0.10	0.05	−0.24	1.06
(97)	MAE	0.91	0.46	0.52	0.60	1.06
total	MSE	−0.78	−0.11	0.04	−0.24	1.01
(115)	MAE	0.90	0.49	0.55	0.62	1.05

[a]The vertical EAs of the EA115 database are evaluated in two different ways.

Table 7. Statistical Errors (in eV) of the Fundamental Gaps for the FG115 Database[28a]

system	error	ωM06-D3	ωB97X-D3	ωB97X-D	ωM05-D	M06-2X
			HOMO−LUMO gaps			
atoms	MSE	−0.36	−1.09	−1.55	−1.14	−2.93
(18)	MAE	0.83	1.36	1.79	1.43	2.93
molecules	MSE	0.34	−0.69	−1.15	−0.62	−2.59
(97)	MAE	0.76	0.73	1.15	0.73	2.59
total	MSE	0.23	−0.75	−1.21	−0.70	−2.64
(115)	MAE	0.77	0.83	1.25	0.84	2.64
			$\varepsilon_{N+1}(N+1)-\varepsilon_N(N)$			
atoms	MSE	−0.82	−0.94	−1.04	−0.95	−0.83
(18)	MAE	0.88	0.99	1.08	0.98	0.87
molecules	MSE	−0.09	−0.35	−0.55	−0.31	−0.42
(97)	MAE	0.46	0.60	0.72	0.56	0.51
total	MSE	−0.21	−0.44	−0.63	−0.41	−0.48
(115)	MAE	0.53	0.66	0.78	0.62	0.57
			IP−EA values			
atoms	MSE	0.28	0.30	0.28	0.28	0.28
(18)	MAE	0.34	0.37	0.36	0.35	0.33
molecules	MSE	0.39	0.26	0.22	0.34	0.28
(97)	MAE	0.45	0.41	0.39	0.44	0.37
total	MSE	0.37	0.27	0.23	0.33	0.28
(115)	MAE	0.43	0.41	0.39	0.43	0.36

[a]The energy gap of each system is evaluated by three different ways.

curves, showing a spurious energy barrier at intermediate bond length R.

4.4. Frontier Orbital Energies. Recently, we proposed the IP131, EA115, and FG115 databases, consisting of accurate reference values for the 131 vertical IPs, 115 vertical EAs, and 115 FGs, respectively, for various atoms and molecules in their experimental geometries.[28] These databases are useful in the assessment of the accuracy of density functional approximations in the prediction of the frontier orbital energies and the fundamental gaps. For the exact KS-DFT, the vertical IP of a neutral molecule is identical to the minus HOMO (highest occupied molecular orbital) energy of the neutral molecule $-\varepsilon_N(N)$,[3,71] and the vertical EA of a neutral molecule is identical to the minus HOMO energy of the anion $-\varepsilon_{N+1}(N+1)$, where $\varepsilon_M(N)$ is the Mth orbital energy of an N-electron system. The vertical EA of a neutral molecule can be approximated by the minus LUMO (lowest unoccupied molecular orbital) energy of the neutral molecule, but it is proved that there exists a difference between the vertical EA and the minus LUMO energy, Δ_{xc}, arising from the discontinuity of exchange-correlation potentials.[72−74] A recent study shows that Δ_{xc} is close to zero for LC hybrid

functionals,[75] so the minus LUMO energy calculated by LC hybrid functionals should be close to the vertical EA.

Here, we evaluate the performance of the functionals on frontier orbital energies for the IP131 and EA115 databases, using the 6-311++G(3df,3pd) basis set and EML(75,302) grid. As shown in Table 6, the minus HOMO energies predicted by the functionals are compared with the accurate vertical IPs of the IP131 database, while each vertical EA of the EA115 database is evaluated in two different ways (by the minus HOMO energy of the anion and by the minus LUMO energy of the neutral molecule). For the IP131 database, ωM06-D3 significantly outperforms others. Overall, LC hybrid functionals are superior to the global hybrid M06-2X, which performs poorly for the HOMO energies due to its incorrect long-range XC-potential behavior.

4.5. Fundamental Gaps. The FG of a system with N electrons is defined as the difference between the vertical IP and EA of the N-electron system. As detailedly described in ref 28, since the IP and EA can both be calculated by their definitions, or by their relations to the frontier orbital energies, there are at least three ways to evaluate a fundamental gap, each requiring one, two, or three self-consistent field (SCF) calculations.

Here, we examine the performance of the functionals on FGs for the FG115 database, using the 6-311++G(3df,3pd) basis set and EML(75,302) grid, with the three different estimates described in ref 28. The results are shown in Table 7, in order of increasing number of SCF calculations required for each molecule. In the estimate requiring three calculations, results are similar for the tested functionals. ωM06-D3 outperforms other functionals in the estimates requiring one or two calculations.

4.6. Long-Range Charge-Transfer Excitations. We perform TDDFT calculations for the lowest charge-transfer (CT) excitation between ethylene and tetrafluoroethylene with a separation of R, following Dreuw et al., who have shown that the exact CT excitation energy from the HOMO of the donor to the LUMO of the acceptor should have the following asymptote:[76]

$$\omega_{CT}(R \to \infty) \approx -\frac{1}{R} + IP_D - EA_A \quad (26)$$

where IP_D is the ionization potential of the donor and EA_A is the electron affinity of the acceptor. High-level results by the symmetry adapted cluster configuration interaction (SAC−CI) method are taken from Tawada et al. for comparison.[16] Figure 3 shows the relative values of the CT excitation energies, in which the curves of the two new functionals are almost overlapped with the accurate curve, and the LC hybrid functionals significantly outperform the global hybrid M06-2X. For the values of CT excitation energies, as shown in Figure 4, ωM06-D3, which is the best functional here, is at least 1 eV better than M06-2X. However, ωM06-D3 and the other LC hybrid functionals are still in error of 1.5 to 2.0 eV, when compared with the reference. Since the LC hybrid functionals are correct at long-range by construction, they still have some short-range SIEs. A more flexible operator for HF exchange may be needed in the LC hybrid functional to reduce such errors.[25]

5. CONCLUSIONS

We have developed two LC hybrid functionals: ωM06-D3 and ωB97X-D3. ωM06-D3 includes 100% long-range HF exchange, a small fraction (about 27%) of short-range HF exchange, a modified M06 exchange density functional for short-range interaction, the M06 correlation density functional, and the empirical dispersion corrections from DFT-D3, while ωB97X-D3, which is reoptimization of ωB97X-D with improved dispersion corrections, includes 100% long-range HF exchange, a small fraction (about 20%) of short-range HF exchange, a modified B97 exchange density functional for short-range interaction, the B97 correlation density functional, and the empirical dispersion corrections from DFT-D3.

Since ωM06-D3 and ωB97X-D3 are parametrized functionals, we test them against three closely related functionals (M06-2X, ωM05-D, and ωB97X-D) on diverse test sets, including further atomization energies, reaction energies, noncovalent interaction energies, energy curves for homonuclear diatomic cation dissociations, frontier orbital energies, fundamental gaps, and a charge-transfer excited state. Both functionals have shown reasonable accuracy over these test sets. Relative to ωB97X-D, ωB97X-D3 provides significant improvement mainly for noncovalent interactions, for its improved dispersion corrections from DFT-D3, while ωM06-D3 shows an overall improvement in performance for a wide range of

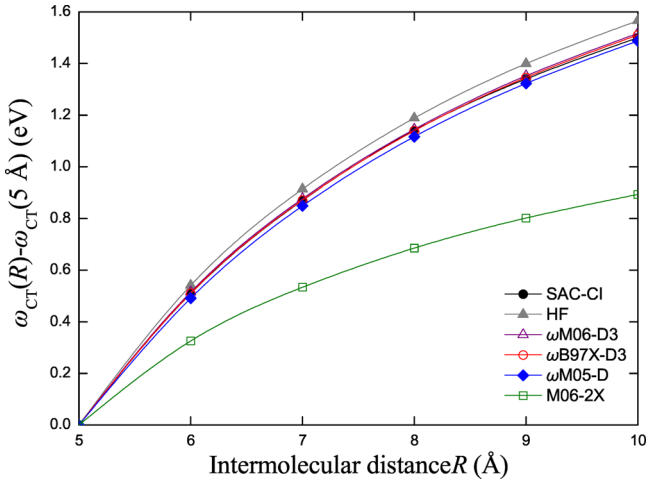

Figure 3. Relative excitation energy for the lowest CT excitation of $C_2H_4\cdots C_2F_4$ dimer along the intermolecular distances R (in Å). The excitation energy at 5 Å is set to zero for each method.

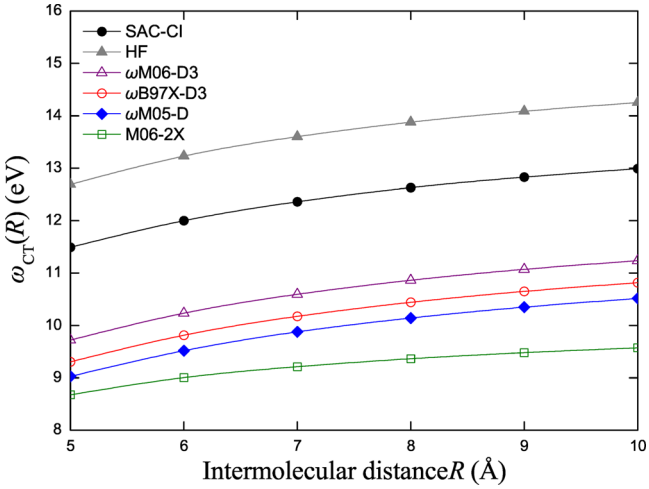

Figure 4. The lowest CT excitation energy of $C_2H_4\cdots$C2F4 dimer along the intermolecular distances R (in Å).

dx.doi.org/10.1021/ct300715s | J. Chem. Theory Comput. 2013, 9, 263−272

applications, possibly for its improved functional form and dispersion corrections.

■ ASSOCIATED CONTENT

Supporting Information

Detailed DFT results for frontier orbital energies, fundamental gaps, atomic energies, barrier heights, reaction energies, and binding energies of noncovalent interactions are provided. This material is available free of charge via the Internet at http://pubs.acs.org/.

■ AUTHOR INFORMATION

Corresponding Author

*E-mail: jdchai@phys.ntu.edu.tw.

Notes

The authors declare no competing financial interest.

■ ACKNOWLEDGMENTS

This work was supported by National Science Council of Taiwan (Grant No. NSC101-2112-M-002-017-MY3), National Taiwan University (Grant Nos. 99R70304, 101R891401, and 101R891403), and National Center for Theoretical Sciences of Taiwan. We are grateful for the partial support of computer resources from the group of Prof. Y.-C. Cheng (NTU).

■ REFERENCES

(1) Hohenberg, P.; Kohn, W. *Phys. Rev.* **1964**, *136*, B864.
(2) Kohn, W.; Sham, L. J. *Phys. Rev.* **1965**, *140*, A1133.
(3) Parr, R. G.; Yang, W. *Density-Functional Theory of Atoms and Molecules*; Oxford University Press: New York, 1989; p 142.
(4) Dreizler, R. M.; Gross, E. K. U. *Density Functional Theory: An Approach to the Quantum Many Body Problem*; Springer-Verlag: Berlin, 1990; p 43.
(5) Engel, E.; Dreizler, R. M. *Density Functional Theory: An Advanced Course*; Springer-Verlag: Berlin, 2011; p 57.
(6) Kohn, W.; Becke, A. D.; Parr, R. G. *J. Phys. Chem.* **1996**, *100*, 12974.
(7) Casida, M. E. In *Recent Advances in Density Functional Methods, Part I*; Chong, D. P., Ed.; World Scientific: Singapore, 1995; p 155.
(8) Gross, E. K. U.; Dobson, J. F.; Petersilka, M. In *Density Functional Theory II*; Nalewajski, R. F., Ed.; Springer: Heidelberg, Germany, 1996; Topics in Current Chemistry Vol. *181*; p 81.
(9) Kümmel, S.; Kronik, L. *Rev. Mod. Phys.* **2008**, *80*, 3.
(10) Perdew, J. P.; Ruzsinszky, A.; Constantin, L. A.; Sun, J.; Csonka, G. I. *J. Chem. Theory Comput.* **2009**, *5*, 902.
(11) Cohen, A. J.; Mori-Sa′nchez, P.; Yang, W. *Chem. Rev.* **2011**, *112*, 289.
(12) Chai, J.-D. *J. Chem. Phys.* **2012**, *136*, 154104.
(13) Becke, A. D. *J. Chem. Phys.* **1993**, *98*, 5648.
(14) Stephens, P. J.; Devlin, F. J.; Chabalowski, C. F.; Frisch, M. J. *J. Phys. Chem.* **1994**, *98*, 11623.
(15) Iikura, H.; Tsuneda, T.; Yanai, T.; Hirao, K. *J. Chem. Phys.* **2001**, *115*, 3540.
(16) Tawada, Y.; Tsuneda, T.; Yanagisawa, S.; Yanai, T.; Hirao, K. *J. Chem. Phys.* **2004**, *120*, 8425.
(17) Gerber, I. C.; Ángyán, J. G. *Chem. Phys. Lett.* **2005**, *415*, 100.
(18) Gerber, I. C.; Ángyán, J. G.; Marsman, M.; Kresse, G. *J. Chem. Phys.* **2007**, *127*, 054101.
(19) Vydrov, O. A.; Heyd, J.; Krukau, A. V.; Scuseria, G. E. *J. Chem. Phys.* **2006**, *125*, 074106.
(20) Vydrov, O. A.; Scuseria, G. E. *J. Chem. Phys.* **2006**, *125*, 234109.
(21) Song, J.-W.; Hirosawa, T.; Tsuneda, T.; Hirao, K. *J. Chem. Phys.* **2007**, *126*, 154105.
(22) Cohen, A. J.; Mori-Sánchez, P.; Yang, W. *J. Chem. Phys.* **2007**, *126*, 191109.
(23) Chai, J.-D.; Head-Gordon, M. *J. Chem. Phys.* **2008**, *128*, 084106.
(24) Chai, J.-D.; Head-Gordon, M. *Phys. Chem. Chem. Phys.* **2008**, *10*, 6615.
(25) Chai, J.-D.; Head-Gordon, M. *Chem. Phys. Lett.* **2008**, *467*, 176.
(26) Chai, J.-D.; Head-Gordon, M. *J. Chem. Phys.* **2009**, *131*, 174105.
(27) Peverati, R.; Truhlar, D. G. *J. Phys. Chem. Lett.* **2011**, *2*, 2810.
(28) Lin, Y.-S.; Tsai, C.-W.; Li, G.-D.; Chai, J.-D. *J. Chem. Phys.* **2012**, *136*, 154109.
(29) Gill, P. M. W.; Adamson, R. D.; Pople, J. A. *Mol. Phys.* **1996**, *88*, 1005.
(30) Dobson, J. F.; McLennan, K.; Rubio, A.; Wang, J.; Gould, T.; Le, H. M.; Dinte, B. P. *Aust. J. Chem.* **2001**, *54*, 513.
(31) (a) Wu, X.; Vargas, M. C.; Nayak, S.; Lotrich, V.; Scoles, G. *J. Chem. Phys.* **2001**, *115*, 8748. (b) Wu, Q.; Yang, W. *J. Chem. Phys.* **2002**, *116*, 515. (c) Zimmerli, U.; Parrinello, M.; Koumoutsakos, P. *J. Chem. Phys.* **2004**, *120*, 2693. (d) Grimme, S. *J. Comput. Chem.* **2004**, *25*, 1463. (e) Grimme, S. *J. Comput. Chem.* **2006**, *27*, 1787. (f) Antony, J.; Grimme, S. *Phys. Chem. Chem. Phys.* **2006**, *8*, 5287. (g) Jurečka, P.; Černý, J.; Hobza, P.; Salahub, D. R. *J. Comput. Chem.* **2006**, *28*, 555. (h) Goursot, A.; Mineva, T.; Kevorkyants, R.; Talbi, D. *J. Chem. Theory Comput.* **2007**, *3*, 755. (i) Grimme, S.; Antony, J.; Schwabe, T.; Mück-Lichtenfeld, C. *Org. Biomol. Chem.* **2007**, *5*, 741. (j) Černy, J.; Jurečka, P.; Hobza, P.; Valdés, H. *J. Phys. Chem. A* **2007**, *111*, 1146. (k) Morgado, C.; Vincent, M. A.; Hillier, I. H.; Shan, X. *Phys. Chem. Chem. Phys.* **2007**, *9*, 448. (l) Kabeláč, M.; Valdés, H.; Sherer, E. C.; Cramer, C. J.; Hobza, P. *Phys. Chem. Chem. Phys.* **2007**, *9*, 5000. (m) Jurečka, P.; Hobza, P. *Phys. Chem. Chem. Phys.* **2007**, *9*, 5291.
(32) Grimme, S.; Antony, J.; Ehrlich, S.; Krieg, H. *J. Chem. Phys.* **2010**, *132*, 154104.
(33) Zhao, Y.; Truhlar, D. G. *Theor. Chem. Acc.* **2008**, *120*, 215.
(34) Zhao, Y.; Truhlar, D. G. *J. Chem. Phys.* **2006**, *125*, 194101.
(35) Zhao, Y.; Truhlar, D. G. *J. Phys. Chem. A* **2006**, *110*, 13126.
(36) Zhao, Y.; Schultz, N. E.; Truhlar, D. G. *J. Chem. Phys.* **2005**, *123*, 161103.
(37) Zhao, Y.; Schultz, N. E.; Truhlar, D. G. *J. Chem. Theory Comput.* **2006**, *2*, 364.
(38) Van Voorhis, T.; Scuseria, G. E. *J. Chem. Phys.* **1998**, *109*, 400.
(39) Henderson, T. M.; Janesko, B. G.; Scuseria, G. E. *J. Chem. Phys.* **2008**, *128*, 194105.
(40) Becke, A. D. *J. Chem. Phys.* **1998**, *109*, 2092.
(41) Perdew, J. P.; Wang, Y. *Phys. Rev. B* **1992**, *45*, 13244.
(42) (a) Stoll, H.; Pavlidou, C. M. E.; Preuss, H. *Theor. Chim. Acta* **1978**, *49*, 143. (b) Stoll, H.; Golka, E.; Preuss, H. **1980**, *55*, 29.
(43) Chakravorty, S. J.; Gwaltney, S. R.; Davidson, E. R.; Parpia, F. A.; Fischer, C. F. *Phys. Rev. A* **1993**, *47*, 3649.
(44) Curtiss, L. A.; Raghavachari, K.; Redfern, P. C.; Pople, J. A. *J. Chem. Phys.* **1997**, *106*, 1063.
(45) Curtiss, L. A.; Redfern, P. C.; Raghavachari, K.; Pople, J. A. *J. Chem. Phys.* **1998**, *109*, 42.
(46) Curtiss, L. A.; Raghavachari, K.; Redfern, P. C.; Pople, J. A. *J. Chem. Phys.* **2000**, *112*, 7374.
(47) Pople, J. A.; Head-Gordon, M.; Fox, D. J.; Raghavachari, K.; Curtiss, L. A. *J. Chem. Phys.* **1989**, *90*, 5622.
(48) Zhao, Y.; Lynch, B. J.; Truhlar, D. G. *J. Phys. Chem. A* **2004**, *108*, 2715.
(49) (a) Zhao, Y.; González-Garca, N.; Truhlar, D. G. *J. Phys. Chem. A* **2005**, *109*, 2012. (b) Zhao, Y.; González-Garca, N.; Truhlar, D. G. *J. Phys. Chem. A* **2006**, *110*, 4942(E).
(50) Jurečka, P.; Šponer, J.; Černý, J.; Hobza, P. *Phys. Chem. Chem. Phys.* **2006**, *8*, 1985.
(51) Takatani, T.; Hohenstein, E. G.; Malagoli, M.; Marshall, M. S.; Sherrill, C. D. *J. Chem. Phys.* **2010**, *132*, 144104.
(52) Marshall, M. S.; Burns, L. A.; Sherrill, C. D. *J. Chem. Phys.* **2011**, *135*, 194102.
(53) Goerigk, L.; Grimme, S. *Phys. Chem. Chem. Phys.* **2011**, *13*, 6670.
(54) Shao, Y.; Fusti-Molnar, L.; Jung, Y.; Kussmann, J.; Ochsenfeld, C.; Brown, S. T.; Gilbert, A. T. B.; Slipchenko, L. V.; Levchenko, S. V.; O'Neill, D. P.; DiStasio, R. A., Jr.; Lochan, R. C.; Wang, T.; Beran, G. J. O.; Besley, N. A.; Herbert, J. M.; Lin, C. Y.; Van Voorhis, T.; Chien, S.

H.; Sodt, A.; Steele, R. P.; Rassolov, V. A.; Maslen, P. E.; Korambath, P. P.; Adamson, R. D.; Austin, B.; Baker, J.; Byrd, E. F. C.; Dachsel, H.; Doerksen, R. J.; Dreuw, A.; Dunietz, B. D.; Dutoi, A. D.; Furlani, T. R.; Gwaltney, S. R.; Heyden, A.; Hirata, S.; Hsu, C.-P.; Kedziora, G.; Khalliulin, R. Z.; Klunzinger, P.; Lee, A. M.; Lee, M. S.; Liang, W.; Lotan, I.; Nair, N.; Peters, B.; Proynov, E. I.; Pieniazek, P. A.; Rhee, Y. M.; Ritchie, J.; Rosta, E.; Sherrill, C. D.; Simmonett, A. C.; Subotnik, J. E.; Woodcock, H. L., III; Zhang, W.; Bell, A. T.; Chakraborty, A. K.; Chipman, D. M.; Keil, F. J.; Warshel, A.; Hehre, W. J.; Schaefer, H. F., III; Kong, J.; Krylov, A. I.; Gill, P. M. W.; Head-Gordon, M. *Phys. Chem. Chem. Phys.* **2006**, *8*, 3172.

(55) Boys, S. F.; Bernardi, F. *Mol. Phys.* **1970**, *19*, 553.

(56) Murray, C. W.; Handy, N. C.; Laming, G. J. *Mol. Phys.* **1993**, *78*, 997.

(57) (a) Lebedev, V. I. *Zh. Vychisl. Mat. Mat. Fiz* **1975**, *15*, 48. (b) Lebedev, V. I. *Zh. Vychisl. Mat. Mat. Fiz* **1976**, *16*, 293. (c) Lebedev, V. I. *Sibirsk. Mat. Zh.* **1977**, *18*, 132.

(58) Boese, A. D.; Martin, J. M. L.; Handy, N. C. *J. Chem. Phys.* **2003**, *119*, 3005.

(59) Curtiss, L. A.; Redfern, P. C.; Raghavachari, K. *J. Chem. Phys.* **2005**, *123*, 124107.

(60) Řezáč, J.; Riley, K. E.; Hobza, P. *J. Chem. Theory Comput.* **2011**, *7*, 2427.

(61) Vydrov, O. A.; Van Voorhis, T. *J. Chem. Theory Comput.* **2012**, *8*, 1929.

(62) (a) Bally, T.; Sastry, G. N. *J. Phys. Chem. A* **1997**, *101*, 7923. (b) Brada, B.; Hiberty, P. C.; Savin, A. *J. Phys. Chem. A* **1998**, *102*, 7872. (c) Mori-Sánchez, P.; Cohen, A. J.; Yang, W. *J. Chem. Phys.* **2006**, *125*, 201102. (d) Ruzsinszky, A.; Perdew, J. P.; Csonka, G. I.; Vydrov, O. A.; Scuseria, G. E. *J. Chem. Phys.* **2007**, *126*, 104102.

(63) Merkle, R.; Savin, A.; Preuss, H. *J. Chem. Phys.* **1992**, *97*, 9216.

(64) Dutoi, A. D.; Head-Gordon, M. *Chem. Phys. Lett.* **2006**, *422*, 230.

(65) Gräfenstein, J.; Kraka, E.; Cremer, D. *J. Chem. Phys.* **2004**, *120* (2), 524.

(66) Gräfenstein, J.; Kraka, E.; Cremer, D. *Phys. Chem. Chem. Phys.* **2004**, *6*, 1096.

(67) Perdew, J. P.; Zunger, A. *Phys. Rev. B* **1981**, *23*, 5048.

(68) Purvis, G. D.; Bartlett, R. J. *J. Chem. Phys.* **1982**, *76*, 1910.

(69) Raghavachari, K.; Trucks, G. W.; Pople, J. A.; Head-Gordon, M. *Chem. Phys. Lett.* **1989**, *157*, 479.

(70) Pan, P.-R.; Lin, Y.-S.; Tsai, M.-K.; Kuo, J.-L.; Chai, J.-D. *Phys. Chem. Chem. Phys.* **2012**, *14*, 10705.

(71) Levy, M.; Perdew, J. P.; Sahni, V. *Phys. Rev. A* **1984**, *30*, 2745.

(72) Sham, L. J.; Schlüter, M. *Phys. Rev. Lett.* **1983**, *51*, 1888.

(73) Sham, L. J.; Schlüter, M. *Phys. Rev. B* **1985**, *32*, 3883.

(74) Perdew, J. P.; Levy, M. *Phys. Rev. Lett.* **1983**, 51.

(75) Tsuneda, T.; Song, J.-W.; Suzuki, S.; Hirao, K. *J. Chem. Phys.* **2010**, *133*, 174101.

(76) Dreuw, A.; Weisman, J. L.; Head-Gordon, M. *J. Chem. Phys.* **2003**, *119*, 2943.